

Statistical laws and self-similarity of vortex rings emitted from a localized vortex tangle in superfluid ^4He

Tomo Nakagawa,¹ Sosuke Inui,¹ Makoto Tsubota,^{1, 2, 3} and Hideo Yano^{1, 2}

¹*Department of Physics, Osaka City University, 3-3-138 Sugimoto, 558-8585 Osaka, Japan*

²*Nambu Yoichiro Institute of Theoretical and Experimental Physics(NITEP),
Osaka City University, 3-3-138 Sugimoto, 558-8585 Osaka, Japan*

³*The Advanced Research Institute for Natural Science and Technology(OCARINA),
Osaka City University, 3-3-138 Sugimoto, 558-8585 Osaka, Japan*

(Dated: February 14, 2020)

We perform numerical simulation of quantum turbulence in superfluid ^4He to observe the emission of vortex rings from a localized vortex tangle. Our goal is to reproduce the two statistical laws that Yano *et al.* observed by vibrating wire experiments [Yano *et al.* *J. Low Temp. Phys.* **196**, 184 (2019)]. The first law is the Poisson process for the detection of vortex rings. This indicated that the vortex tangle emits vortex rings with frequencies depending on their size. The second law is the power law between the frequency and the size of the vortex rings emitted from the vortex tangle. This law shows that the tangle has self-similarity. To confirm these laws numerically, we develop a system similar to the experiments. First, we generate a localized statistically steady vortex tangle by injecting vortex rings from two opposite sides and making them collide with each other, and we study the conditions in which the tangle develops and the anisotropy of the emission of vortex rings from the tangle. Second, by taking the statistics of the emitted rings, we reproduce the two statistical laws. These numerical studies confirm the self-similarity of the emitted vortex rings and the localized tangle.

I. INTRODUCTION

Quantum turbulence refers to turbulent states in quantum condensed fluids. This is an important problem not only in low temperature physics but also in other fields such as fluid mechanics and non-equilibrium physics. Superfluid ^4He is a typical system where quantum turbulence is studied. Many researchers have investigated it for more than half a century [1–4]. Statistical laws are often investigated to determine the universal properties of turbulence. In classical turbulence, one of the most important statistical laws is Kolmogorov’s law that the energy spectrum follows $-5/3$ power law of the wave number [5, 6], which shows self-similarity in wave number space. In real space, the self-similarity is also expected to be typically like the Richardson cascade that large-sized eddies can split into smaller sizes [5, 6]. Eddies or vortices should be responsible for the self-similarity and cascade of turbulence. However, it is difficult to understand the self-similarity and cascade of classical turbulence in real space because vortices are unstable and not well-defined.

Quantum turbulence and quantized vortices have an advantage over classical turbulence and vortices. In superfluid ^4He , vortices are stable topological defects and their circulation is conserved by quantization to be the quantum of circulation $\kappa = h/m$, where h and m are Planck’s constant and the mass of a ^4He atom [7, 8]. Since quantum turbulence consists of such well-defined elements, studies can provide a shortcut for understanding turbulence. The self-similarity of quantum turbulence in wave number space such as Kolmogorov’s law has been studied [9–17]. However, the self-similarity in the real space has not been studied much except for several works [13, 18, 19]. We focus on the statistical laws

in the real space assuming that quantum turbulence has some self-similarity.

Liquid ^4He makes the transition to superfluid phase below $T_\lambda = 2.17$ K, and its hydrodynamics is described by the two-fluid model. It means that superfluid ^4He is a mixture of a viscous normal fluid component and an inviscid superfluid component [20, 21]. The density and velocity of the superfluid component are ρ_s , \mathbf{v}_s , and those of the normal fluid component are ρ_n , \mathbf{v}_n . The total density is $\rho = \rho_s + \rho_n$. The ratio ρ_s/ρ increases as the temperature decreases, and particularly, below approximately 1 K, the ratio is $\rho_s/\rho \simeq 1$. At finite temperatures, mutual friction works between two components through quantized vortices. One of the important actions of mutual friction is to shrink a vortex ring that moves in the fluid.

There are several ways to generate quantum turbulence in superfluid ^4He [1–3], and experiments using oscillating objects have been conducted as a powerful method recently [22–33]. A vibrating wire is a typical oscillating object. Thin wires are vibrated by Lorentz force under a static magnetic field, and turbulence is generated around the wire. Yano *et al.* have conducted a series of experiments using vibrating wires [24, 29, 33, 34]. The advantage of the Yano group is to discover two kinds of vibrating wires, namely, a generator of turbulence and detector of vortices. A generator wire has remnant vortices, while a detector wire is free of remnant vortices. The wire velocity increases with the driving force, but two kinds of wires behave completely differently. When the driving force exceeds some critical value, the velocity of the generator wire decreases suddenly and a vortex tangle is generated around it. However, a detector wire never generates turbulence by itself because of the success of removing remnant vortices around it. When a vortex

ring approaches a detector wire, however, it generates a vortex tangle around it using the ring as a trigger and the wire velocity decreases. In this manner, Yano *et al.* performed experiments using a detector wire to detect the vortex rings emitted from a vortex tangle made by a generator wire.

One of the most important features of this experiment is that it is possible to control the minimum size of detectable vortex rings by changing the temperature. At zero temperature, a vortex ring moves with its self-induced velocity without shrinking. While at finite temperatures, a vortex ring shrinks during its flight and may thus fade away through mutual friction. The flight distance l until a vortex ring with an initial radius R_0 disappears is given by $l = R_0/\alpha$, where α is the mutual friction coefficient described later. Thus, the diameter $2R_0$ of a detectable vortex ring satisfies $2R_0 > 2\alpha D$, where D is the distance between the detector and the generator wires.

Using the setup, Yano *et al.* recently succeeded in observing some self-similarity of vortices emitted from a vortex tangle. This experiment found mainly two things. First, the time of the flight of vortex rings from the vortex tangle to the detector wire follows exponential distribution for any detectable minimum size. In other words, the detection of vortex rings follows the Poisson process. It means that vortex rings are detected with frequencies depending on their sizes, namely, the vortex tangle is in a statistically steady state. Second, the vortex tangle has self-similarity. In this experiment, they found the relationship between the detection frequency and the minimum size of the detectable vortex rings that satisfies the power law. The vortex ring size should reflect the vortex line spacings in the tangle. Thus, we expect that the vortex tangle has a self-similar structure in the real space.

In the experiments of quantum turbulence generated by oscillating objects, several numerical simulations have also been conducted. The purpose of previous simulations was to reveal the mechanism of growth and decay of a localized vortex tangle or the anisotropy of the emission of vortex rings from the tangle [34–37]. However, this study focuses on the statistical laws and the self-similarity of the vortex ring emission from a localized tangle, which differs from the previous works.

By using the vortex filament model, we study numerically the dynamics and statistics of the vortices emitted from a vortex tangle. First, we obtain a localized statistically steady vortex tangle as the source of emitted vortex rings. Second, we study the statistics of the vortex rings emitted from the tangle. In Section II, we introduce the vortex filament model and the system treated in this study. Next, we investigate how the vortex tangle develops in Section III. In Section IV, we discuss a statistically steady vortex tangle and introduce theoretical aspects. Then, we reproduce two statistical laws in Section V. Finally, Section VI presents the conclusions.

II. THE MODEL AND SYSTEM

A. Vortex filament model

Quantized vortices in superfluid ^4He are stable topological defects with quantized circulation and thin cores of the order of 1 Å. Therefore, we can use the vortex filament model in which vortices are treated like filaments. The superfluid velocity field obtained due to quantized vortices is given by the Biot-Savart law [38]

$$\mathbf{v}_{s,BS}(\mathbf{r},t) = \frac{\kappa}{4\pi} \int_L \frac{\mathbf{s}'(\xi,t) \times (\mathbf{r} - \mathbf{s}(\xi,t))}{|\mathbf{r} - \mathbf{s}(\xi,t)|^3} d\xi. \quad (1)$$

Here, $\mathbf{s}(\xi,t)$ is the position of the vortex filaments represented by a parameter ξ , and \mathbf{s}' is $\frac{\partial \mathbf{s}}{\partial \xi}$. The integration is performed over the whole vortex filaments L . At finite temperatures, mutual friction affects the motion of vortices. When there are neither boundaries nor applied superfluid flow, the equation of motion becomes

$$\frac{d\mathbf{s}}{dt} = \mathbf{v}_{s,BS} + \alpha \mathbf{s} \times (\mathbf{v}_n - \mathbf{v}_{s,BS}) - \alpha' \mathbf{s}' \times [\mathbf{s}' \times (\mathbf{v}_n - \mathbf{v}_{s,BS})], \quad (2)$$

where α and α' are the coefficients of friction depending on the temperature. In particular, we have $\alpha, \alpha' = 0$ at $T = 0$ K.

The vortex lines are discretized into a number of points held at a minimum space resolution $\Delta\xi = 0.8 \mu\text{m}$. The integration in time is performed using the fourth-order Runge-Kutta scheme, in which the time resolution is $\Delta t = 10 \mu\text{s}$. We use the traditional method to artificially reconnect two vortices that approach each other within $\Delta\xi$ [39]. We delete the vortex rings whose lengths are shorter than $6\Delta\xi$.

B. The system

The motivation of this work is to reproduce the statistical laws observed by the experiments and reveal the self-similarity of the system. For this purpose, we first obtain a localized stationary vortex tangle as the source and then observe the emission of vortex rings from the tangle.

How to make a localized vortex tangle is a key issue of our simulation. We are mainly interested in the emission of vortex rings from a localized vortex tangle. Thus, we use a novel method that is different from the previous simulations [34–37] to generate a dense localized vortex tangle that can emit many vortex rings. As shown in Fig. 1, we virtually prepare two parallel $100 \mu\text{m} \times 100 \mu\text{m}$ square vortex sources that inject vortex rings with a certain size at a fixed frequency from random positions in each square. The distance between two injectors is $240 \mu\text{m}$. The only parameters of this simulation are the injection frequency f and the diameter $2R_0$ of the injected vortex rings. Now, we take f on the order of 1 kHz,

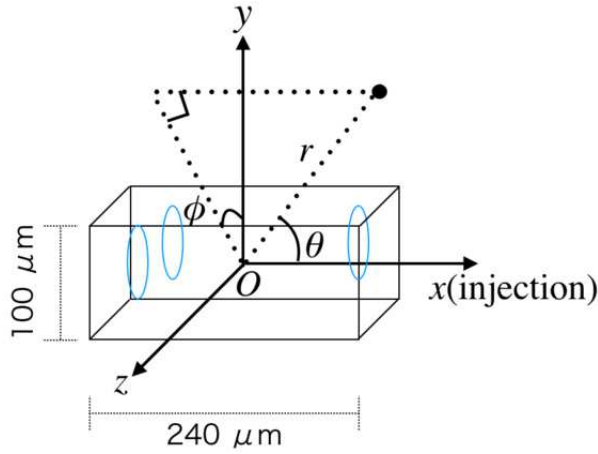


FIG. 1. The coordinate system of this system. We set x axis injection direction of vortex rings. Vortex rings are injected from two parallel $100\mu\text{m} \times 100\mu\text{m}$ square vortex sources at a fixed frequency.

which corresponds to the frequency of the vibrating wire and $2R_0$ on the order of $10\mu\text{m}$, which is the amplitude of the vibration [33]. As described later, we keep injecting vortices from two sources and generate a localized vortex tangle between them. This tangle tends to expand orthogonally to the direction of the injection, as shown in Fig. 2. This tangle can be regarded as a source vortex tangle created by a vibrating object.

The next task is to simulate the detection of vortices by the detector. The experiment prepared one detector and repeated the observations to obtain the statistical law [33]. Instead our simulation allocates many detectors around the tangle. The vortex tangle and the emitted vortex rings should be symmetric about the azimuthal angle ϕ . The vortex rings tend to be emitted orthogonally to the direction of injection, as described in the next section. We collect the data of the vortex rings emitted from a vortex tangle at a fixed distance of $400\mu\text{m}$ from the origin and analyze it.

III. PROPERTIES OF THE LOCALIZED VORTEX TANGLE

On comparison with the experiments [33], the success of this simulation depends on whether we can obtain a statistically steady localized vortex tangle by the method described in the last section. In this section, we describe the development of the vortex tangle and shows that a statistically steady vortex tangle can be generated. Then, we describe the statistics of the observation of the vortex rings emitted from a vortex tangle.

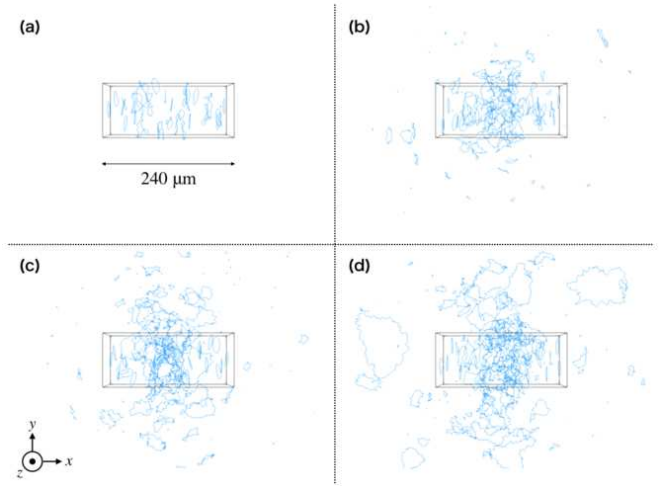


FIG. 2. Development of vortex tangle in $f = 1000\text{ Hz}$ and $2R_0 = 30\mu\text{m}$ at time (a) $t = 0.02\text{ s}$ (b) $t = 0.06\text{ s}$ (c) $t = 0.16\text{ s}$ (d) $t = 0.40\text{ s}$, respectively. The black rectangular box refers to the box in Fig. 1. Vortex tangles of (a) and (b) grow, but those of (c) and (d) are saturated inside the box.

A. Development of vortex tangle

Figure 2 shows the typical development of the vortex tangle. When vortex rings begin to be injected from the vortex sources, they make the small nucleus of a vortex tangle around the origin if they frequently collide with each other (See supplemental material). Then, the nucleus absorbs the following vortex rings, which grows the vortex tangle. This explanation seems reasonable, but it is not so trivial that the resulting localized vortex tangle becomes statistically steady or not.

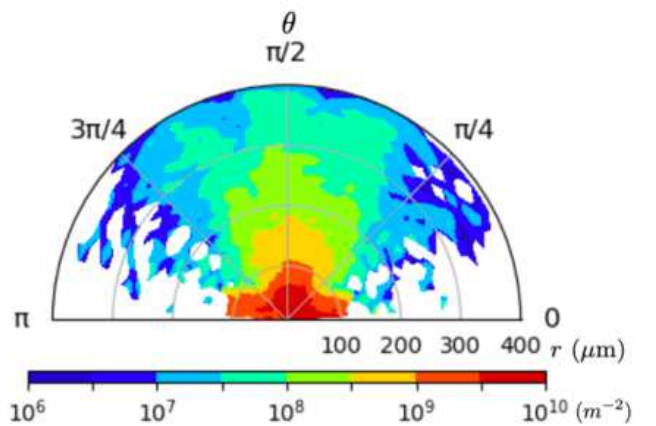


FIG. 3. The time averaged($t=0.4\text{--}0.6\text{ s}$) distribution of the vortex line density (m^{-2}) of the vortex tangle in a $r(\mu\text{m}) - \theta(\text{rad})$ plane in the log scale. The condition is $f = 1000\text{ Hz}$ and $2R_0 = 30\mu\text{m}$. Since the vortex tangle is symmetric around the azimuthal angle ϕ , the distribution is obtained by integrating over ϕ .

Figure 3 shows the vortex line density distribution after the tangle develops enough and seems to be statistically steady. As the distance from the origin increases, the density decreases. The density is concentrated around $\theta = \frac{\pi}{2}$ because of the symmetry of the system.

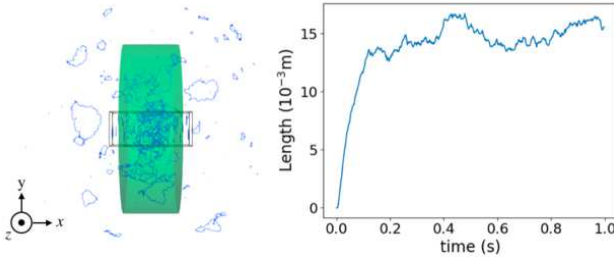


FIG. 4. The vortex line length in the cylindrical volume in $2R_0 = 30 \mu\text{m}$ and $f = 1000 \text{ Hz}$. The cylindrical volume has its height $160 \mu\text{m}$ and its radius $250 \mu\text{m}$. This cylinder covers the vortex tangle. The black box in the left figure is as same as that in Fig. 2. The figure on the right shows development of the vortex line length. After about $t = 0.1 \text{ s}$, it becomes statistically steady.

Next, we try to investigate properties of the tangle more directly. The vortex distribution in Fig. 3 includes emitted vortex rings as well as a localized tangle. From Fig. 3, we know that the tangle expands orthogonally to x axis and the approximate size of the tangle. Then, we assume a cylindrical volume with height $160 \mu\text{m}$ and radius $250 \mu\text{m}$ which covers the vortex tangle and reflects its symmetry. The centroid of the volume is placed at the origin, and the bottom is orthogonal to the x axis. Figure 4 shows the development of the total vortex line length in the cylindrical volume. The vortex line length increases with time and becomes statistically steady after about $t = 0.1 \text{ s}$.

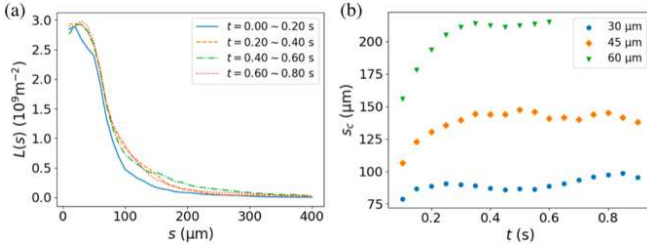


FIG. 5. (a) The time averaged vortex line density distribution in $f = 1000 \text{ Hz}$ and $2R_0 = 30 \mu\text{m}$. The colors represent the distribution averaged over the different time intervals. (b) The time development of s_c in $f = 1000 \text{ Hz}$. The colors represent the different injected vortex ring sizes $2R_0$. The time interval over which the density is averaged for $t - 0.1 \text{ s} \sim t + 0.1 \text{ s}$.

In order to characterize its steady state, we investigate the distribution $L(s)$ of the vortex line density in hollow cylindrical volumes with height, inner radius, and outer

radius as $160 \mu\text{m}$, $s - ds$, and s , respectively. The centroid of the volume is placed at the origin, and the bottom is orthogonal to the x axis. Figure 5(a) shows the time-averaged distribution $L(s)$. Since the distribution does not change much after about $t = 0.2 \text{ s}$, the tangle is found to be statistically steady about the vortex distribution as well as the its total length.

From the distribution of the vortices, we try to estimate the size of the tangle, although there is some arbitrariness for defining the size of the tangle. We define the tangle size s_c such that the density $L(s)$ decreases to 10^{-9} m^{-2} in the volume.

Figure 5(b) shows the time development of s_c for $2R_0 = 30, 45, 60 \mu\text{m}$ and $f = 1000 \text{ Hz}$. The tangle size seems to converge to a finite value in each condition. The size of tangle in the statistically steady state increases with $2R_0$.

It is not so trivial whether the vortex tangle develops and becomes statistically steady or not. The injected vortex rings are shuffled to form a localized vortex tangle. The vortex tangle emits vortex rings, which works as the dissipation for the tangle. The statistically steady state is sustained by the equilibrium between the vortex ring injection and the vortex ring emission from the tangle. We do not know whether such statistical steady states are always obtained for arbitrary values of $2R_0$ and f . This topic will be a future work.

B. The vortex line length of vortex tangle

If the injection frequency f and the size $2R_0$ of the injected vortex rings are reduced, a statistically steady vortex tangle may not be generated because vortex rings do not frequently collide with each other and generate no nucleus of a tangle.

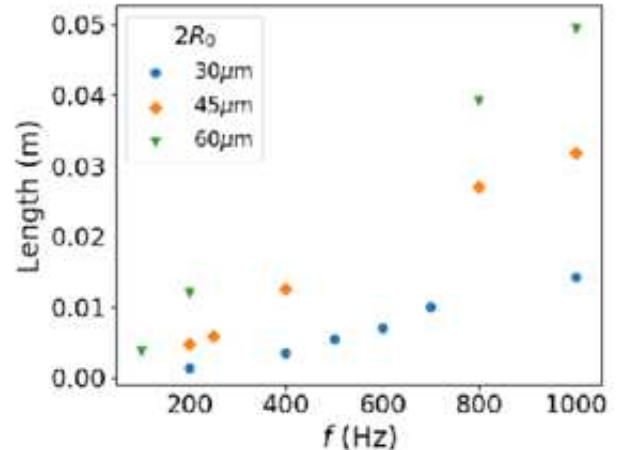


FIG. 6. The mean vortex line length in the cylindrical volume. The horizontal axis is the frequency f .

We calculate the dynamics with varying f and $2R_0$ to study the condition that a statistically steady vortex

tangle is generated. Figure 6 shows that the statistically steady vortex line length in the cylinder increases with f and $2R_0$.

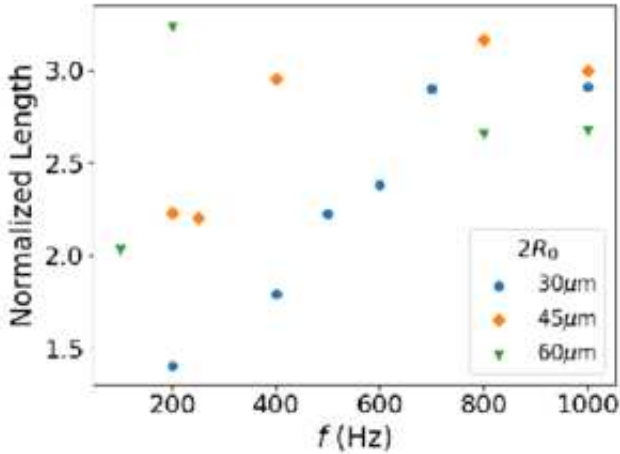


FIG. 7. The vortex line length normalized by $16\pi^2 lf R_0^2 / (\kappa \log(R_0/r_c))$ which is the length when the vortex rings never collide with each other. Here $2R_0$ and l are the size of injected vortex rings and the height of the cylindrical volume, respectively.

Whether a nucleus of a vortex tangle appears or not decides its growth. If no nucleus is formed, no vortex tangle occurs. Investigating the condition of the formation of a nucleus enables us to determine the characteristic vortex length. If the injected vortex rings collide and interact with each other, the vortex length increases. We consider the vortex length when counter-propagating rings pass through and no nucleus is formed. This consideration gives us the characteristic vortex length, by which we normalize the vortex line length in the cylinder. This characteristic length can be given by considering the geometry of Fig. 1. When counter-propagating vortex rings never collide, we can obtain the time $4\pi l R_0 / (\kappa \log(R_0/r_c))$ that it takes for an injected ring to pass through the cylindrical volume because of the self-induced velocity of the vortex ring $v \sim \kappa / 4\pi R_0 \times \log(R_0/r_c)$. Here, l is the height of the cylindrical volume. Since the length of the injected vortex rings is $2\pi R_0$, the desirable length is $2 \times f \times 4\pi l R_0 / (\kappa \log(R_0/r_c)) \times 2\pi R_0 = 16\pi^2 lf R_0^2 / (\kappa \log(R_0/r_c))$. The vortex line length normalized by this characteristic length is shown in Fig. 7. This quantity is the amplification factor of the vortex line length. When the normalized length exceeds unity, the mere group of ballistic vortex rings develops to a vortex tangle. As the injected vortex ring size and the frequency of the injection increase, the length increases, and converges to about 3 independently of $2R_0$ as f increases. This means that the vortex line length is proportional to $f R_0^2$.

C. Emission of vortex rings from a vortex tangle

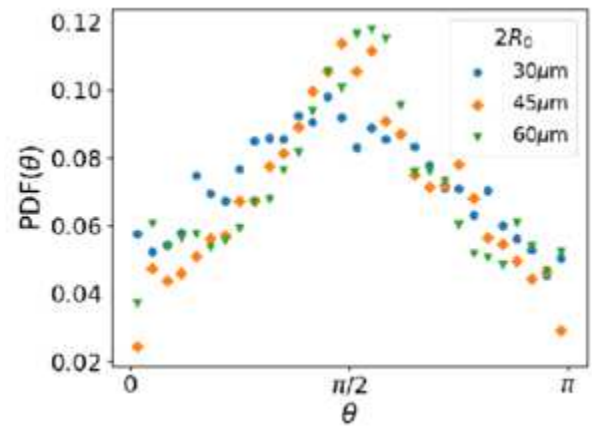


FIG. 8. The probability density function, $\text{PDF}(\theta)$, of the direction of the emitted vortex rings about θ . The PDF is obtained from the number of vortex rings caught by the detectors within $2\pi \sin \theta d\theta$.

The distribution of the emitted vortex rings is isotropic about ϕ , but that in the direction θ is anisotropic. The probability density function(PDF) of the direction θ of the vortex rings emitted from the vortex tangle is shown in Fig. 8. The data of the vortex rings are collected by the detectors placed at $400 \mu\text{m}$ from the origin. The emission of the vortex rings is concentrated around $\theta = \frac{\pi}{2}$.

IV. STATISTICALLY STEADY TANGLE

A statistically steady vortex tangle should emit vortex rings of each size with the corresponding frequency, namely, the emission frequency of a certain size obeys the function $f(R)$ that depends only on the vortex ring size R . This statistically steady picture is the key of this study. Our simulation finds that $f(R)$ is a power of R , that is, the emission of the vortex rings from a tangle has some self-similarity. We introduce the theoretical aspects of this self-similarity in this section.

A. Poisson process

To observe the statistics of emitted vortex rings, the experiment is conducted assuming the Poisson process [33]. The Poisson process is a stochastic process based on an exponential distribution. First, we describe how to derive the process considering the situation of the experiment. We suppose the following. A detector catches n vortex rings in the time interval $[0, T]$, which is divided by the small interval Δt . Thus, the probability that a vortex ring is detected during Δt is $\Delta t \frac{n}{T}$. This is based

on an assumption that Δt is so small that the number of vortex rings caught during Δt is 0 or 1. The probability that a vortex ring is not detected in $[0, t]$ and detected in $[t, t + \Delta t]$ is

$$\left(1 - \Delta t \frac{n}{T}\right)^{\frac{t}{\Delta t}} \times \Delta t \frac{n}{T}. \quad (3)$$

If $P(t)$ is the probability that a vortex ring is detected in $[0, t]$, we have

$$P(t + \Delta t) - P(t) = \left(1 - \Delta t \frac{n}{T}\right)^{\frac{t}{\Delta t}} \times \Delta t \frac{n}{T}. \quad (4)$$

The PDF $F(t)$ is defined by the probability $F(t)dt$ that a vortex ring is detected in $[t, t + \Delta t]$. Then, $F(t)$ is obtained as

$$F(t) = \lim_{\Delta t \rightarrow 0} \frac{P(t + \Delta t) - P(t)}{\Delta t} = \frac{1}{t_1} \exp\left(-\frac{t}{t_1}\right). \quad (5)$$

Here $t_1 \equiv \frac{T}{n}$ is the mean detection interval. Finally, integrating $F(t)$ yields

$$P(t) = \int_0^t F(t')dt' = -\exp\left(-\frac{t}{t_1}\right) + 1 \quad (6)$$

and

$$1 - P(t) = \exp\left(-\frac{t}{t_1}\right). \quad (7)$$

This indicates the Poisson process. If this relation is confirmed, the interval t_1 is constant, which means that the vortex tangle is statistically steady and emits vortex rings continuously and steadily. Yano *et al.* observed this relation, which means that the generator wire generates a statistically steady vortex tangle [33]. This is the reason why we try to obtain a statistically steady vortex tangle in the present simulation.

B. The self-similarity

We consider that the vortex tangle has self-similarity in real space, and we find the power law between the emission frequency and the vortex ring size. The experiment observed the power law [33]. This self-similarity is understood by the following discussions. We define the number $n(x, t)dx$ of vortex rings with the diameter $x \sim x + dx$ emitted from the tangle during $[0, t]$. The number $N_{2R>2R_C}(t)$ of the vortex rings with diameters larger than $2R_C$ emitted during $[0, t]$ is $N_{2R>2R_C}(t) = \int_{2R_C}^{\infty} n(x, t)dx$. Because the vibrating wire experiments observe only vortex rings larger than some minimum size, we also consider the number of vortex rings larger than some minimum size. When the vortex tangle is statistically steady, the number of emitted rings $n(x, t)dx$ is shown by $g(x)tdx$ and emits vortex rings with various

size. Here, $g(x)dx$ is the emission frequency of the vortex rings with size $x \sim x + dx$. Therefore, the frequency $f_{2R>2R_C}$ of the emission of rings larger than $2R_C$ is

$$f_{2R>2R_C} = \int_{2R_C}^{\infty} g(x)dx. \quad (8)$$

The distribution of vortices in the tangle should be reflected by that of the emitted vortex rings. Several literatures have reported the size distribution of vortex rings in a tangle, which shows that the number of vortex rings decreases with the ring size by some power law [13, 18]. Assuming the emission of the vortex rings is self-similar, the frequency $g(x)$ can be written as $g(x) = x^{-\alpha}$, which yields

$$f_{2R>2R_C} = \int_{2R_C}^{\infty} x^{-\alpha} dx \propto (2R_C)^{-\alpha+1}. \quad (9)$$

Thus, the power law comes from the self-similarity of the size distribution of the vortex rings in the tangle.

V. STATISTICAL LAWS

We describe the statistical laws of the vortex rings emitted from a vortex tangle. The first law is the Poisson process of the detection of the vortex rings emitted from a tangle. The second is the power law between the frequency of the emission and the vortex ring size.

The statistically steady vortex tangle emits vortex rings, as mentioned in Section IV. In this section, we study numerically the probability that the detectors catch vortex rings larger than a certain minimum diameter $2R$. Experiments are performed by one detector and the observations are repeated to take statistics. Instead, our simulation replaced it with just one simulation caught by 2000 detectors.

A. Poisson process

We prepare detectors at a fixed distance of $400 \mu\text{m}$ from the origin and orthogonal to the x axis as shown in Fig. 9. In this study, the number of detectors N_{det} is 2000. The simulation indicates the number $N(t)$ of detectors that catch at least one vortex ring in $[0, t]$. The probability $P(t)$ is given by

$$P(t) = N(t)/N_{\text{det}}. \quad (10)$$

This relation is the key idea that relates our simulation to the experiment.

Figure 10 shows the results of the simulation in $f = 1000 \text{ Hz}$ and $2R_0 = 30$. They support Eq. (7) clearly such that our simulation reproduces the Poisson process observed experimentally. These slopes indicate the detection frequencies t_1^{-1} .

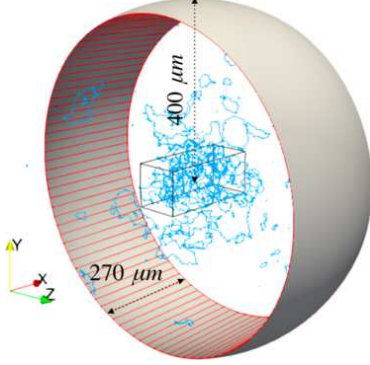


FIG. 9. The schematic figure of the arrangement of the detectors around the vortex tangle. The detectors are arranged symmetrically with the width $270 \mu\text{m}$

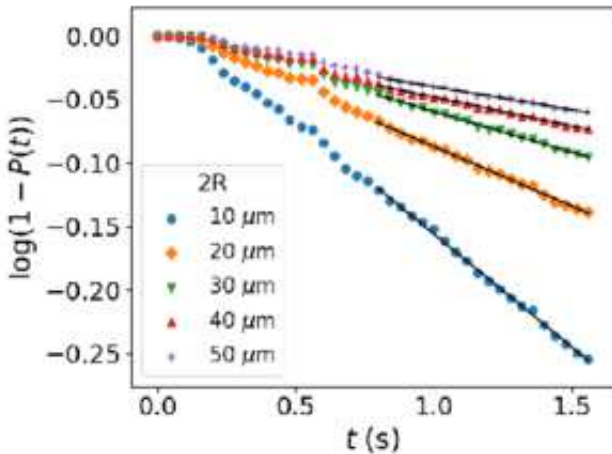


FIG. 10. The time development of $1 - P(t)$ in $f = 1000 \text{ Hz}$ and $2R_0 = 30 \mu\text{m}$. Here, $2R$ refers to the minimum size of detectable vortex rings.

To investigate the property of the vortex tangle more directly, we investigate the emission frequency as well. Figure 11 shows the number $N_{\text{emi}}(t)$ of vortex rings that are larger than $2R$ and emitted in $[0, t]$. We can confirm the linear relationship $N_{\text{emi}}(t) = t/t_1$ with the emission frequency t_1^{-1} . This figure shows that the frequency becomes constant, which means that the vortex tangle becomes statistically steady.

B. The power law

The power law between t_1^{-1} and $2R$ means the self-similarity of the vortex rings emitted from the localized vortex tangle. Figure 12 shows that the emission frequency t_1^{-1} obeys the power law of $2R$ for three different values of $2R_0$. In the case of $f = 1000 \text{ Hz}$ and $2R_0 = 30 \mu\text{m}$, the power law $t_1^{-1} = (2R)^{-1.03}$ is obtained by the least square method. Therefore, we can obtain results

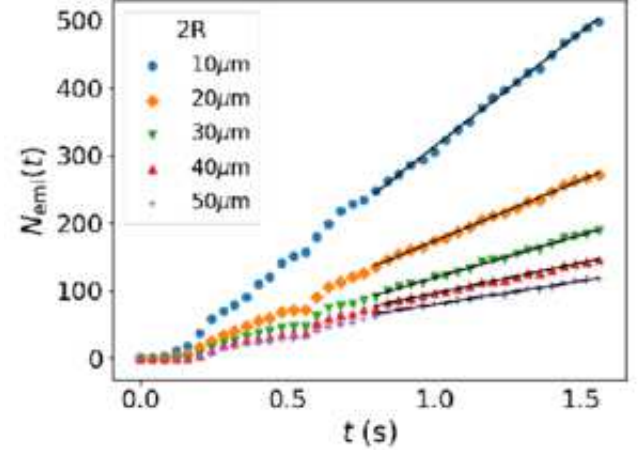


FIG. 11. The number $N(t)$ of the vortex rings emitted in $[0, t]$. The frequency of emission converges at finite number in each minimum size. Here, $2R$ refers to the minimum size of detectable vortex rings.

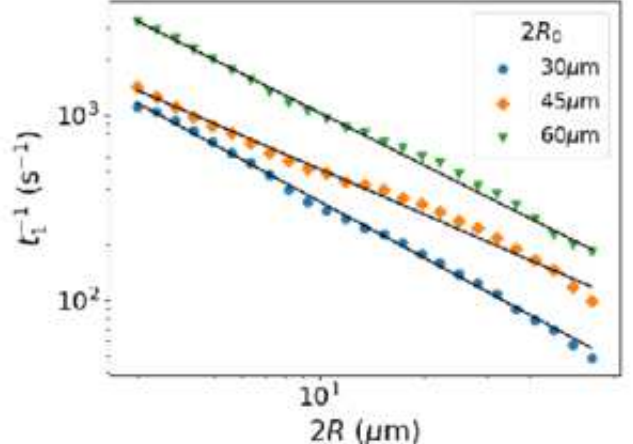


FIG. 12. The relationship between t_1^{-1} and $2R$ in the log-log scale.

similar to the experiments. Here, we determine the slope in the range up to $60 \mu\text{m}$ because the data above $60 \mu\text{m}$ (not shown in Fig. 11) are deviated from the power law. This deviation may come from the rare events catching such large vortices. This result shows that the distribution vortex rings emitted from the localized vortex tangle has self-similarity, which may reflect the self-similarity of the vortex size distribution of a vortex tangle.

Finally, we compare the power exponent obtained by this study with that obtained through the experiments. In the experiments, the exponent depends on the turbulence generation power. Yano *et al.* observed that the exponents increased to -2.5 , -1.6 , and -1.5 as the power increases to 40 pW , 150 pW and 1000 pW , respectively. Whereas our simulation shows the power exponents $-0.86 \sim -1.03$, which are different from the ex-

perimental results because the vortices become too dense to be calculated numerically.

The difference in the exponents between the simulation and the experiments may relate to the injected power. The energy ϵ of the vortex filaments per unit length is $\epsilon = \frac{\rho_s \kappa^2}{4\pi} \ln \left(\frac{R_{cv}}{r_c} \right) \sim 1.25 \times 10^{-12} \text{ J/m}$. Thus, the energy injected per unit time is $2\pi R_0 \times f \times \epsilon \sim 10^{-1} \text{ pW}$. The order of injected energy in this study is much lower than that in the experiments. Unfortunately, it is numerically difficult to increase the power to make it comparable with the experiments.

VI. CONCLUSION

We investigated numerically the emission of vortex rings from a statistically steady localized vortex tangle, which was formed by making vortex rings colliding with each other. Our aim was to reproduce the statistical laws that Yano *et al.* observed through the vibrating wire experiments [33]. The laws showed two important properties of a statistically steady vortex tangle. First, the vortex tangle emits vortex rings with frequencies depending on their size. Second, the vortex tangle emits vortex rings self-similarly.

In this study, we performed simulations at $T = 0 \text{ K}$,

while the experiments were performed at finite temperatures. The advantage of performing the simulation at 0 K is that the vortex rings do not shrink spontaneously at 0 K, so it is easy to fix the sizes of the vortex rings emitted from the tangle. However, at finite temperatures, the mutual friction shrinks the vortex rings, whose size is not determined easily.

Therefore, it is ideal to perform the simulation at finite temperatures. There are mainly two methods to realize it. The first method is traditional, namely, following the vortex dynamics under the prescribed normal fluid velocity [38]. This is relatively easy to calculate, and it is a future plan. The second is to consider the fully coupling dynamics between a normal fluid component and a superfluid component [40–42]. This is better than the first method. However, it is very difficult to calculate the fully coupled dynamics for the present problem.

Our next work will investigate the self-similar structure of the vortex tangle, such as a fractal dimension [43], and associate it with the statistical laws of the emitted vortex rings addressed in this paper.

ACKNOWLEDGMENTS

M. T. acknowledges the support from JSPS KAKENHI (Grant No. JP17K05548). H. Y. acknowledges the support from JSPS KAKENHI (Grant No. 15H03694).

[1] W. F. Vinen and J. J. Niemela, *J. Low Temp. Phys.* **128**, 167 (2002).
[2] M. Tsubota, M. Kobayashi, and H. Takeuchi, *Physics Reports* **522**, 191 (2013), quantum hydrodynamics.
[3] C. F. Barenghi, L. Skrbek, and K. R. Sreenivasan, *PNAS* **111**, 4647 (2014).
[4] M. Tsubota, K. Fujimoto, and S. Yui, *J. Low Temp. Phys.* **188**, 119 (2017).
[5] P. A. Davidson, *turbulence :An Introduction for Science and Engineers* (Oxford University Press, 2004).
[6] U. Frisch, *Turbulence: The Legacy of A. N. Kolmogorov* (Cambridge University Press, 1995).
[7] R. Feynman (Elsevier, 1955) pp. 17 – 53.
[8] W. F. Vinen, *Proc. R. Soc. Lond. A* **260** (1961).
[9] C. Nore, M. Abid, and M. E. Brachet, *Phys. Rev. Lett.* **78**, 3896 (1997).
[10] C. Nore, M. Abid, and M. E. Brachet, *Phys. Fluids* **9**, 2644 (1997).
[11] J. Maurer and P. Tabeling, *Europhys. Lett.* **43**, 29 (1998).
[12] S. R. Stalp, L. Skrbek, and R. J. Donnelly, *Phys. Rev. Lett.* **82**, 4831 (1999).
[13] T. Araki, M. Tsubota, and S. K. Nemirovskii, *Phys. Rev. Lett.* **89**, 145301 (2002).
[14] M. Kobayashi and M. Tsubota, *Phys. Rev. Lett.* **94**, 065302 (2005).
[15] M. Kobayashi and M. Tsubota, *J. Phys. Soc. Jpn.* **74**, 3248 (2005).
[16] N. G. Parker and C. S. Adams, *Phys. Rev. Lett.* **95**, 145301 (2005).
[17] A. W. Baggaley, J. Laurie, and C. F. Barenghi, *Phys. Rev. Lett.* **109**, 205304 (2012).
[18] A. Mitani and M. Tsubota, *Phys. Rev. B* **74**, 024526 (2006).
[19] T. Kadokura and H. Saito, *Phys. Rev. Fluids* **3**, 104606 (2018).
[20] L. Tisza, *Nature* **141**, 913 (1938).
[21] L. Landau, *Phys. Rev.* **60**, 356 (1941).
[22] J. Jäger, B. Schuderer, and W. Schoepe, *Phys. Rev. Lett.* **74**, 566 (1995).
[23] J. Luzuriaga, *J. Low Temp. Phys.* **108**, 267 (1997).
[24] H. Yano, N. Hashimoto, A. Handa, M. Nakagawa, K. Obara, O. Ishikawa, and T. Hata, *Phys. Rev. B* **75**, 012502 (2007).
[25] N. Hashimoto, R. Goto, H. Yano, K. Obara, O. Ishikawa, and T. Hata, *Phys. Rev. B* **76**, 020504 (2007).
[26] D. Garg, V. B. Efimov, M. Giltrow, P. V. E. McClintock, L. Skrbek, and W. F. Vinen, *Phys. Rev. B* **85**, 144518 (2012).
[27] D. I. Bradley, S. N. Fisher, A. M. Guénault, R. P. Haley, V. Tsepelin, G. R. Pickett, and K. L. Zaki, *J. Low Temp. Phys.* **154**, 97 (2009).
[28] D. Bradley, M. Fear, S. Fisher, A. Gunault, R. Haley, C. Lawson, P. McClintock, G. Pickett, R. Schanen, V. Tsepelin, and L. Smethurst, *J. Low Temp. Phys.* **156**, 116 (2009).
[29] H. Yano, Y. Nago, R. Goto, K. Obara, O. Ishikawa, and

T. Hata, Phys. Rev. B **81**, 220507 (2010).

[30] D. I. Bradley, A. M. Guénault, S. N. Fisher, R. P. Haley, M. J. Jackson, D. Nye, K. O’Shea, G. R. Pickett, and V. Tsepelin, J. Low Temp. Phys. **162**, 375 (2011).

[31] D. I. Bradley, M. Človečko, S. N. Fisher, D. Garg, E. Guise, R. P. Haley, O. Kolosov, G. R. Pickett, V. Tsepelin, D. Schmoranz, and L. Skrbek, Phys. Rev. B **85**, 014501 (2012).

[32] D. I. Bradley, S. N. Fisher, A. M. Guénault, R. P. Haley, M. Kumar, C. R. Lawson, R. Schanen, P. V. E. McClintock, L. Munday, G. R. Pickett, M. Poole, V. Tsepelin, and P. Williams, Phys. Rev. B **85**, 224533 (2012).

[33] H. Yano, K. Sato, K. Hamazaki, R. Mushiake, K. Obara, and O. Ishikawa, J. Low Temp. Phys. **196**, 184 (2019).

[34] R. Goto, S. Fujiyama, H. Yano, Y. Nago, N. Hashimoto, K. Obara, O. Ishikawa, M. Tsubota, and T. Hata, Phys. Rev. Lett. **100**, 045301 (2008).

[35] R. Hänninen, M. Tsubota, and W. F. Vinen, Phys. Rev. B **75**, 064502 (2007).

[36] S. Fujiyama, A. Mitani, M. Tsubota, D. I. Bradley, S. N. Fisher, A. M. Guénault, R. P. Haley, G. R. Pickett, and V. Tsepelin, Phys. Rev. B **81**, 180512 (2010).

[37] A. Nakatsuji, M. Tsubota, and H. Yano, Phys. Rev. B **89**, 174520 (2014).

[38] K. W. Schwarz, Phys. Rev. B **31**, 5782 (1985).

[39] H. Adachi, S. Fujiyama, and M. Tsubota, Phys. Rev. B **81**, 104511 (2010).

[40] D. Kivotides, C. F. Barenghi, and D. C. Samuels, Science **290**, 777 (2000).

[41] D. Kivotides, Phys. Rev. B **76**, 054503 (2007).

[42] S. Yui, M. Tsubota, and H. Kobayashi, Phys. Rev. Lett. **120**, 155301 (2018).

[43] D. Kivotides, C. F. Barenghi, and D. C. Samuels, Phys. Rev. Lett. **87**, 155301 (2001).